# Determining surface Fermi level pinning position of InN nanowires using electrolyte gating

D. R. Khanal,[1,2] W. Walukiewicz,[2] J. Grandal,[3] E. Calleja,[3] and J. Wu[1,2,a)]
[1]*Department of Materials Science and Engineering, University of California, Berkeley, California 94720, USA*
[2]*Materials Science Division, Lawrence Berkeley National Laboratory, Berkeley, California 94720, USA*
[3]*Department of Ingeniería Electrónica-ISOM, Universidad Politécnica, Ciudad Universitaria, Madrid, Spain*

(Received 29 July 2009; accepted 6 October 2009; published online 30 October 2009)

We demonstrate quantitative determination of surface Fermi level pinning position in InN nanowires using polymer electrolyte gating and three-dimensional (3D) electrostatic modeling of charge distribution. We find pinning of the Fermi level 0.6–0.7 eV above the conduction band minimum at the surface of the nanowires. After taking into account the Fermi level pinning, doping concentration and carrier mobilities are also evaluated and compared with InN thin films. This general approach of combining electrolyte gating experiments with 3D numerical modeling can be applied to nanowires of other materials to determine their surface Fermi level pinning position. © *2009 American Institute of Physics*. [doi:10.1063/1.3255010]

Surface Fermi level pinning has long been a major issue for semiconductor technology. Despite displacement of the Fermi level ($E_F$) in the bulk of a semiconductor by extrinsic doping, the surface or interface $E_F$ can remain pinned at a particular energy with respect to the band edges due to a high density of surface or interface states that trap charges and induce an electric field near the surface region. The characteristic distance required to screen this electric field, the Debye screening length, is typically on the order of tens of nanometers. This means the majority of the material is unaffected for bulk semiconductors, but nanoscale semiconductors such as nanowires can have the majority of their volume be under the influence of this internal electric field. Thus, surface $E_F$ pinning can have dramatic effects on the electronic properties of nanoscale semiconductors.

Unfortunately, measuring band bending in nanowires and other nanoscale semiconductors is not straightforward. In III-nitride nanowires, for example, the existence of surface $E_F$ pinning has so far been only indirectly deduced. In GaN nanowires, reports show a sharp increase in nanowire resistance below a certain diameter, suggesting near mid-gap pinning of $E_F$ at the surface.[1] In InN nanowires, conductivity scaling with diameter has been used to suggest the existence of a surface electron accumulation layer,[2,3] corresponding to a pinning of $E_F$ above the conduction band minimum.[4] Unfortunately, these techniques do not quantify the level of band bending in the nanowires. That is, the thickness and charge distribution of the band-bending shell in the nanowires are unknown. As a result, contributions to electrical conduction from the core and shell cannot be accurately decoupled. A more quantitative analysis of the band profile in nanowires is lacking.

Methods of quantifying band bending in semiconductors typically involve applying an external gating electric field to modulate the band bending and measuring a resultant change in current or capacitance. The most accessible of these techniques is the transconductance or field-effect transistor (FET) measurement, where the free carrier concentration in the channel is modulated by the gating field via the gate-channel capacitance. As the gating field is varied, the conductivity of the channel is measured, which is proportional to the product of carrier mobility ($\mu$) and concentration ($n$). As the capacitance of a single nanowire is difficult to measure,[5] $\mu$ and $n$ are typically decoupled by analytically *calculating* the capacitance between the gate and the channel. As we[6] and others[7] have shown, for nanoscale semiconductor devices, numerical electrostatic modeling is often required to accurately determine the gate-channel capacitance depending on the gate geometry. Since surface $E_F$ pinning significantly affects the carrier distribution in nanowires and thus influences channel conductivity, if it is included in the electrostatic modeling, the surface $E_F$ pinning position can be deduced by fitting to the measured transconductance data.

In this paper, we use InN nanowires as a model material system and a polymer-based electrolyte as the gating medium to demonstrate extraction of the surface $E_F$ pinning position from transconductance measurements. We also show that this method of taking into account band bending in analyzing the transconductance data yields more precise estimates for ionized dopant concentration and free carrier mobility of the nanowires. InN is an ideal material to study the band bending effect because its $E_F$ at the surface is pinned at a very high energy above the conduction band minimum (~0.9 eV) (Refs. 8 and 4) in all polar (c-plane) and nonpolar (a/m-plane) films exposed to ambient.[9] This property, combined with the propensity of native defects to dope InN n-type, makes unintentionally doped InN nanowires display heavily n-type characteristics and makes them difficult to fully deplete with a conventional back-gate; a higher dielectric constant or tighter gating geometry such as an electrolyte gate is required to achieve larger gating capacitance.[10,11] We also note that studying single-crystal nanowires avoids the complication in thin film experiments of differentiating between effects of the film surface from the film-substrate interface.[10]

a)Electronic mail: wuj@berkeley.edu.

 

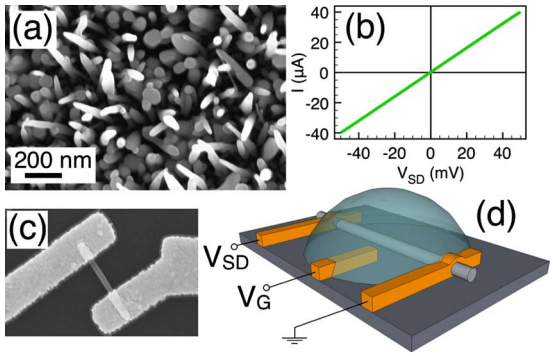


FIG. 1. (Color online) (a) Top-down SEM image of as-grown InN nanowires. (b) $I$-$V_{SD}$ curve of a typical InN nanowire device. (c) SEM of a nanowire contacted with Ti/Au electrodes (nanowire diameter is 50 nm). (d) Schematic of the electrolyte gating setup. Semitransparent hemisphere is the electrolyte.

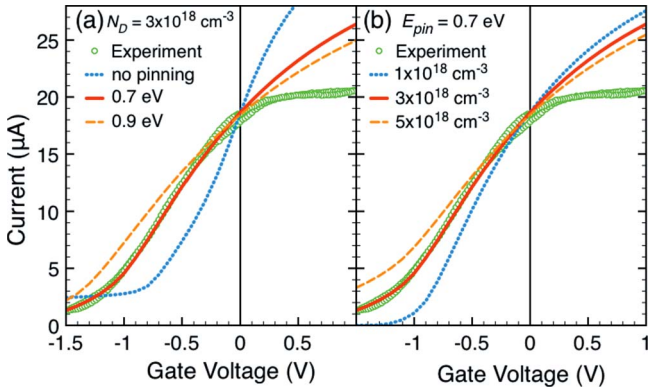


FIG. 2. (Color online) (a) Experimental $I$-$V_G$ curves from an InN nanowire (27.5 nm radius) along with simulated $I$-$V_G$ curves assuming an $N_D$ concentration of $3\times10^{18}$ cm$^{-3}$ and $E_{pin}$ values of no pinning ($\mu$=1600 cm$^2$/V s), 0.7 eV ($\mu$=340 cm$^2$/V s), and 0.9 eV ($\mu$=240 cm$^2$/V s). (b) Same experimental $I$-$V_G$ as (a) with simulated curves assuming $E_{pin}$=0.7 eV and $N_D$ values of $1\times10^{18}$ cm$^{-3}$ ($\mu$=440 cm$^2$/V s), $3\times10^{18}$ cm$^{-3}$ ($\mu$=340 cm$^2$/V s), and $5\times10^{18}$ cm$^{-3}$ ($\mu$=280 cm$^2$/V s).

InN nanowires were grown by plasma-assisted molecular beam epitaxy on (100) Si substrates. The nanowires grow in the c-direction (thus have non-polar sidewalls), show clear hexagonal facets [Fig. 1(a)], and are free of extended defects as detailed in a previous publication.[12] Nanowires were transferred from their growth substrate onto SiN (200 nm)/Si chips by the standard drop-casting technique. Ti/Au contacts were patterned by electron-beam lithography and deposited by electron beam evaporation after an $O_2$ plasma treatment (70 W/30 s) to remove organic surface contaminants [Fig. 1(c)].

All devices measured showed linear $I$-$V_{SD}$ behavior with resistances on the order of kilohms, corresponding to conductivities in the range of 700 to 2300 $(\Omega\ \mathrm{cm})^{-1}$, which is typical of InN nanowires [Fig. 1(b)].[2,13,14] Extrapolating the resistance of over 30 devices (not shown) to zero length, we obtained a contact resistance of 440 $\Omega$, which is non-negligible compared to the lowest resistance in some of the nanowires and must be included in the modeling as discussed.[15]

A schematic of the electrolyte gating setup is shown in Fig. 1(d). A small source-drain voltage ($V_{SD}$) was applied across the nanowire to monitor the current while a third, gate electrode was used to modulate the potential of the polymer electrolyte relative to source-drain, The electrolyte is $KClO_4^-$ in 1000 MW polyethylene oxide (PEO) with a [K]:[O] ratio of 100:1.[16] When a positive (negative) voltage ($V_G$) is applied to the gate electrode, cations (anions) in the electrolyte migrate to the nanowire surface and induce negative (positive) charges inside the nanowire channel. At sufficiently low gate voltages, this process happens without appreciable exchange of charge (leakage current) between the ions in the electrolyte and the semiconductor nanowire. In this way, the electrolyte gate is electrostatically analogous to a solid surround gate with a gate dielectric thickness equal to the solvation shell of the ions in the electrolyte ($\sim$1 nm).[16]

Figure 2 shows a typical $I(V_G)$ curve of the InN nanowires. $V_G$ was scanned from 0 to $-1.5$ V, and then back to +1 V at a slow scan rate of 4 m V/s. At faster scan rates the $I(V_G)$ curves developed wide hysteresis and we were unable to deplete the nanowire completely, which is likely due to slow diffusivity of ions[17] to and from the surface of the nanowire.

Using electrostatic simulations as discussed above, $I(V_G)$ curves were computed for different ionized donor concentrations ($N_D$) and surface $E_F$ pinning positions. Current was calculated using a standard Drude model of conductivity, allowing the electron concentration, $n$, to be a function of radial position across the nanowire,

$$I(V_G) = \frac{2\pi V_{SD}}{L} e\mu \int_0^R r \cdot n(r, V_G) dr, \tag{1}$$

where $L$ is the length and $R$ is the radius of the nanowire channel. The contact resistance, $R_C$, shifts $V_{SD}$ by an amount of $I \cdot R_C$, which was also taken into account.[15] Note that holes do not contribute to current even if they are induced, because the $E_F$ pinning at the ungated InN-electrode interface blocks collection and injection of holes.[18]

The radial electron distribution, $n(r, V_G)$, as a function of $V_G$ was computed by solving the Poisson equation[11] in three dimensions using finite-element modeling software (COMSOL MULTIPHYSICS) for the surround-gate FET geometry as detailed in Ref. 6. The nonparabolicity[4] of the InN conduction band was also included in calculating the conduction band density of states. The relative dielectric constant of InN (Ref. 4) and PEO (Ref. 16) were set to 10.5 and 10, respectively.

The initial surface $E_F$ pinning position ($E_{pin}$) is the energy of $E_F$ relative to the conduction band minimum at the surface. In the simulation, $E_{pin}$ was adjusted by varying the fixed surface charge concentration on the nanowire, which, for InN, is positive and induces a surface accumulation of free electrons on the order of $10^{12}$ cm$^{-2}$ even at zero $V_G$.[11] For a given $N_D$ and $E_{pin}$, the Poisson equation was solved for a range of $V_G$. The resulting $n(r, V_G)$ was then substituted into Eq. (1) to give $I(V_G)$ curves for each combination of $N_D$ and $E_{pin}$. The mobility ($\mu$) used for each $I(V_G)$ curve was that which made the simulated curve agree with the experimental current at $V_G$=0. The simulated and experimental $I(V_G)$ curves were then compared to find the values of $N_D$ and $E_{pin}$ that best fit the experimental data.

Figure 2(a) shows the effect of $E_{pin}$ on $I(V_G)$ for a given $N_D$ ($3\times10^{18}$ cm$^{-3}$). The three $E_{pin}$ curves are representative of the range of $E_{pin}$ values tested for each nanowire, from no surface $E_F$ pinning to $E_{pin}$=0.9 eV. Figure 2(a) shows that the best fit is achieved with an $E_{pin}$ in between the two extremes, at approximately $E_{pin}$=0.7 eV. The flattening out of the simulated $I(V_G)$ curves at positive $V_G$ is due to the inclu-

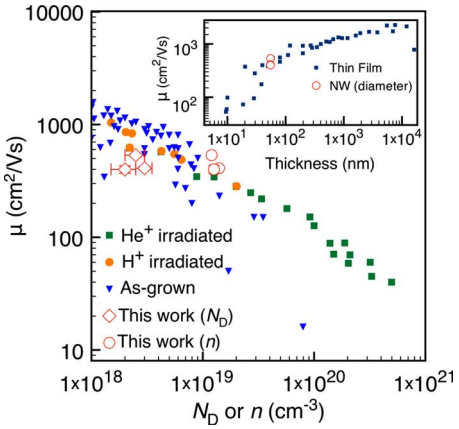


FIG. 3. (Color online) Mobility vs electron or donor concentration of InN thin films from Ref. 20 plotted with mobilities of three InN nanowires of radii $26 \pm 1.5$ nm studied in this work. Inset: mobility vs thickness of InN thin films from Ref. 21 plotted with mobility vs diameter of these three nanowires.

sion of contact resistance in Eq. (1). However, this limiting of current by contact resistance is still insufficient to fit the experimental curve at positive $V_G$. Similar current saturation in heavy-accumulation regions has been reported before in polymer electrolyte gated FETs, though the exact mechanism is not clear.[17] Figure 2(b) shows the effect of varying $N_D$ on $I(V_G)$ with $E_{pin}$ held at 0.7 eV. We see that the fit is quite sensitive to the background donor concentration and the best fit at this particular value of $E_{pin}$ is $3 \times 10^{18}$ cm$^{-3}$.

This analysis was performed on three nanowires with radii of ~26 nm and found $E_{pin}$ values of (0.6–0.7 eV), $N_D$ values of $(2 \times 10^{18} - 4 \times 10^{18}$ cm$^{-3})$, and mobilities of (400–550 cm$^2$/V s). We note that the $E_{pin}$ range determined for the nanowires is slightly lower than is commonly reported for InN thin films (0.9 eV).[4] It has been suggested that nonpolar planes of InN could display $E_F$ pinning at lower energies with respect to the conduction band minimum than the polar c-plane.[19] However, we also note that this discrepancy can be attributed to the limited accuracy of the material parameters used in the simulations, most notably the relative dielectric constants of the electrolyte and semiconductor.

The mobilities obtained fall within a much narrower range than previous reports.[2,14] We compare the mobility values of these three nanowires with Hall mobilities of InN thin films[20,21] in Fig. 3. The nanowire mobilities agree with mobilities for InN thin films with similar $N_D$, with slightly lower values due possibly to the small diameter of nanowires (Fig. 3, inset). This agreement suggests that electron mobility in InN nanowires is also limited by scattering from charged point defects, similar to InN thin films.[20] Lastly, we note that calculating a mobility from the data in Fig. 2 through the conventional method[14] of measuring the slope of the $I$-$V_G$ curve and using an analytical expression for a surround gate capacitance $(C = 2\pi\varepsilon L / \ln[(R+h)/R])$,[6] we obtain a mobility of 195 cm$^2$/V s, which is more than a factor of 2 lower than the mobility calculated from our numerical modeling (550 cm$^2$/V s). This difference arises from the erroneous estimate of the total gate-channel capacitance with the analytical equation, which completely ignores the contribution to capacitance from band bending inside the semiconductor nanowire.[6] More importantly, the free electron concentration (between 1 and $5 \times 10^{19}$ cm$^{-3}$, determined at zero $V_G$ using either of the above mobilities) originates from both ionized donors ($N_D$) and $E_{pin}$-induced band bending. If the effect of the surface $E_F$ pinning is ignored, all electrons would be attributed to $N_D$, and $N_D$ would be severely over-estimated as shown in Fig. 3. This analysis highlights the importance of band bending effects and surface $E_F$ pinning in considering the electronic properties of semiconductor nanowires and the performance of nanowire devices.

In summary, we have performed field-effect transistor measurements on InN nanowires using a polymer electrolyte gate, and taking this system as an example, provided a strategy for quantitative estimate of the surface Fermi level pinning position in the nanowires through numerical electrostatic modeling. We also report improved estimation of the doping level and electron mobility that takes into account the band bending in these nanowires. The analysis is of general importance as it can be applied to understanding the electrostatic effects of the surface on the electronic properties of other nanomaterial systems.

We acknowledge help from Raymond Zhong, Gregory F. Brown, Tyler Matthews, and Dr. D. F. Ogletree. This work was supported in part by National Science Foundation under Grant No. EEC-0425914, and in part by the Laboratory Directed Research and Development Program of Lawrence Berkeley national laboratory (LBNL) under the Department of Energy under Contract No. DE-AC02-05CH11231. Part of the work was performed at the Molecular Foundry, LBNL.

[1] R. Calarco, M. Marso, T. Richter, A. I. Aykanat, R. Meijers, A. d. Hart, T. Stoica, and H. Lüth, Nano Lett. **5**, 981 (2005).
[2] F. Werner, F. Limbach, M. Carsten, C. Denker, J. Malindretos, and A. Rizzi, Nano Lett. **9**, 1567 (2009).
[3] E. Calleja, J. Grandal, M. A. Sánchez-García, M. Niebelschutz, V. Cimalla, and O. Ambacher, Appl. Phys. Lett. **90**, 262110 (2007).
[4] J. Wu, J. Appl. Phys. **106**, 011101 (2009).
[5] E. C. Garnett, Y. Tseng, D. R. Khanal, J. Wu, J. Bokor, and P. Yang, Nat. Nanotechnol. **4**, 311 (2009).
[6] D. R. Khanal and J. Wu, Nano Lett. **7**, 2778 (2007).
[7] O. Wunnicke, Appl. Phys. Lett. **89**, 083102 (2006).
[8] I. Mahboob, T. D. Veal, C. F. McConville, H. Lu, and W. J. Schaff, Phys. Rev. Lett. **92**, 036804 (2004).
[9] P. D. C. King, T. D. Veal, C. F. McConville, F. Fuchs, J. Furthmuller, F. Bechstedt, P. Schley, R. Goldhahn, J. Schoermann, D. J. As, K. Lischka, D. Muto, H. Naoi, Y. Nanishi, H. Lu, and W. J. Schaff, Appl. Phys. Lett. **91**, 092101 (2007).
[10] G. F. Brown, J. W. Ager, W. Walukiewicz, W. J. Schaff, and J. Wu, Appl. Phys. Lett. **93**, 262105 (2008).
[11] J. W. L Yim, R. E. Jones, K. M. Yu, J. W. Ager, W. Walukiewicz, W. J. Schaff, and J. Wu, Phys. Rev. B **76**, 041303(R) (2007).
[12] J. Grandal, M. A. Sanchez-Garcia, F. Calle, and E. Calleja, Phys. Status Solidi C **2**, 2289 (2005).
[13] C. Y. Chang, G. C. Chi, W. M. Wang, L. C. Chen, K. H. Chen, F. Ren, and S. J. Pearton, Appl. Phys. Lett. **87**, 093112 (2005).
[14] Z. Cai, S. Garzon, M. V. S. Chandrashekhar, R. A. Webb, and G. Koley, J. Electron. Mater. **37**, 585 (2008).
[15] S. A. Dayeh, D. P. R. Aplin, X. Zhou, P. K. L. Yu, E. T. Yu, and D. Wang, Small **3**, 326 (2007).
[16] K. Ueno, S. Nakamura, H. Shimotani, A. Ohtomo, N. Kimura, T. Nojima, H. Aoki, Y. Iwasa, and M. Kawasaki, Nature Mater. **7**, 855 (2008).
[17] M. J. Panzer and C. D. Frisbie, J. Am. Chem. Soc. **129**, 6599 (2007).
[18] R. E. Jones, K. M. Yu, S. X. Li, W. Walukiewicz, J. W. Ager, E. E. Haller, H. Lu, and W. J. Schaff, Phys. Rev. Lett. **96**, 125505 (2006).
[19] D. Segev and C. G. van de Walle, Europhys. Lett. **76**, 305 (2006).
[20] R. E. Jones, S. X. Li, L. Hsu, K. M. Yu, W. Walukiewicz, Z. Lillental-Weber, J. W. Ager, E. E. Haller, H. Lu, and W. J. Schaff, Physica B **376**, 436 (2006).
[21] W. J. Schaff, X. Chen, D. Hao, K. Matthews, T. Richards, L. F. Eastman, H. Lu, C. J. Cho, and H. Y. Cha, Phys. Status Solidi B **245**, 868 (2008).